CHEMICAL ENGINEERING TRANSACTIONS

VOL. 100, 2023

A publication of AIDIC

The Italian Association of Chemical Engineering
Online at www.cetjournal.it

Guest Editors: Sauro Pierucci, Flavio Manenti

ISBN 979-12-81206-03-8; **ISSN** 2283-9216

DOI: 10.3303/CET23100026

Characterization of Powder Flowability for Additive Manufacturing

Silvia Volpato*, Andrea C. Santomaso

APTLab-Advanced ParticleTechnology Laboratory, Department of Industrial Engineering, University of Padova, Italy
s.volpato@aptlab.it

Powders have always been used in industry, spanning from food to metallurgic ones, and in recent decades they have become the protagonists of other innovative process: additive manufacturing (AM).
Knowing the flowability of a powder in a specific piece of equipment is fundamental to achieve better manufacturing efficiency and product quality in powder processing industries. A powder used in AM machines is subjected to different flow and stress regimes. There are commercial devices able to measure the flowability of the powder under different levels of consolidation stresses, but they are not able to work at very low stresses. Among the available, alternative, non-commercial tests dynamic BIM is the most promising. In dynamic BIM a spherical indenter impinges on the powder with the velocity of a falling body; it is possible to determine the flowability (through the hardness) of the powder, but the evaluation is complex and must be improved.
In this work we investigate the dynamic impact of an indenter in a packed powder, measuring the geometrical characteristic of the crater forming on the powder surface. Furthermore, we try to improve the definition of dynamic hardness and shear rate by rewriting them in terms of granular velocity rather than indenter impact velocity as the most common reports in the literature.

1. Introduction

Powders are widely used in industry and in recent decades they have become the protagonists of another innovative process: additive manufacturing (AM). Additive manufacturing is a generic term to indicate industrial processes used to construct 3D objects, directly from Computer-Aided Design (CAD) files, by depositing material layer upon layer. Among the AM processes, powders are used as input material in the Directed Energy Deposition and Powder Bed Fusion. These processes use powders in different ways but they have one thing in common: the efficiency of the process depends on how the powder flows.
The propensity of a powder to flow is called flowability. Knowing the flowability of a powder in a specific piece of equipment is fundamental for achieving better manufacturing efficiency and product quality in powder processing industries. A powder used in AM machines is subjected to different flow and stress regimes.
There are commercial devices able to measure the flowability of the powder under different levels of stress, but all of them are not able to investigate systems with very low (less than 1 kPa) stresses. Also when dealing with cohesive powders, where even small variations in inter-particle contact forces have a large effect, these testers do not reproduce the initial state of filling reliably and reproducibly (Zafar et al., 2015)
A new promising method used to measure the flowability is the *Ball Indentation Method* (BIM), able to give information on the flowability of a powder both in quasi-static conditions (very low deformation rate) or in dynamic conditions (high deformation rate). The method was already used to evaluate the flowability of powder (Pasha et al., 2015; Zafar et al., 2015) but to complete the study is necessary to find a clear correlation between flowability, consolidation of material, grains properties (size, shape, friction, particle density), and bulk properties (bulk density, cohesion).

Paper Received: 17 January 2023; Revised: 20 March 2023; Accepted: 28 May 2023
Please cite this article as: Volpato S., Santomaso A.C., 2023, Characterization of Powder Flowability for Additive Manufacturing, Chemical Engineering Transactions, 100, 151-156 DOI:10.3303/CET23100026

The method, which consists of indenting the surface of a pre-consolidated powder bed with a ball, allows the material hardness, *H*, which is defined as the resistance of the material to plastic deformation, to be determined. The indentation can be quasi-static or dynamic. With quasi-static indentation the indenter is driven at a constant rate, the penetration depth is controlled and the loading force is measured. Whereas with the dynamic approach, the indenter is released and accelerates under gravity. The penetration depth cannot be controlled in this case: it depends on the indenter kinetic energy and powder flow properties.
In this work, we reported the data obtained with the method of dynamic ball indentation. We calculated the dynamic hardness of the powder moving in the intermediate flow regime using a new equation and verified the reliability of an already used fitting expression (Tirapelle et al., 2022) using a different definition of shear rate. Furthermore, we will show a first attempt to link the dynamic hardness with the packing fraction of the granular bed.

2. Materials and methods

2.1 Materials

The powder used in dynamic indentation experiments was sodium bicarbonate. The equivalent diameter of this material, d_p=0.095 mm, was calculated from the averaged value of the particle size distribution obtained from sieve analysis. The intrinsic density of sodium bicarbonate is equal to 2200 kg/m^3.
The dynamic hardness measurements were done with a customized device whose configuration requires a magnet and a high-definition camera. The consolidated state of the powder was verified by measuring the powder bulk density. The powder was poured into a cup with a known volume (25 cm^3), and weighed, and the ratio between the powder weight and the cup volume returned the average bulk density value. Then the indenter, which is initially held by the electromagnet above the sample at a controlled variable height, is released by switching off the electromagnet. The use of the electromagnet guarantees the repeatability of the test and the consistency of the results. By placing the indenter at different heights, different impact velocities were investigated. The impact of the indenter on the powder was recorded with SvPro Camer. By post-processing image analysis of the frames, the height of indenter penetration, *h*, and the radius R_C of the crater created on the powder surface were determined as sketched in Figure 1.

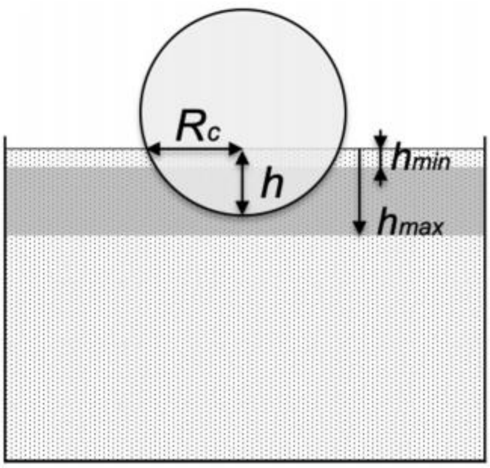

Figure 1: Geometrical quantities determinable from the impact of the indenter on the powder (Tirapelle, 2020).

Two different spherical indenters made of steel, differing in diameters, were used in the experiments: D_i=6 and 8 mm. The intrinsic density of both the indenters was 7684 kg/m^3.
For characterizing the flow behavior of the powder, a powder flowability test was performed with a shear cell (PFT Powder Flow Tester, AMETEK Brookfield, USA). According to the classification of powder flowability introduced by Jenike [22], sodium bicarbonate displays an easily flowing behavior.

2.2 Method

The resistance of the powder in the static indentation is calculated using the static hardness, the ratio between the maximum load, $F_{max,}$ and the area of penetration, *A* (Hassanpour and Ghadiri, 2007):

$$H_s = \frac{F_{max}}{A} \quad (1)$$

In dynamic indentation, instead, the hardness is typically calculated from the energy balance, assuming that all the energy of the impacting ball is dissipated in the plastic deformation of the target material (Tirupataiah and Sundararajan, 1991):

$$H_d = \frac{m_i v_i^2}{U} \quad (2)$$

where m_i is the mass of the indenter, v_i is its impact velocity on powder and *U* is the unrelaxed crater volume:

$$U = \frac{h\pi}{6}(3R_C^2 + h^2) \quad (3)$$

The indenter impact velocity is:

$$v_i = \sqrt{(2gh_d)} \quad (4)$$

where h_d is the indenter dropping height.
From a specific energy balance, it is also possible calculated the powder velocity:

$$v_g = v_i\left(\frac{\rho_i}{\rho_b}\right)^{0.5} \quad (5)$$

that depends on the level of consolidation of the power through the bulk density,ρ_b,on the impact velocity of the ball and on the density of the indenter ρ_i.
In this work, we calculate the dynamic hardness using the powder velocity as following:

$$H_d = \frac{m_i v_i^2}{U}\left(\frac{\rho_i}{\rho_b}\right) \quad (6)$$

Also the shear rate was reformulated in terms of granular velocity (instead of indenter impact velocity as previously done (Tirapelle et al., 2020; Pasha et al., 2015)):

$$\dot{\gamma} = \frac{v_g}{D_i} \quad (7)$$

where D_i is the diameter of the indenter. Later in the paper, it will be possible to see that determination of the shear rate using the powder velocity instead of impact velocity as done by Tirapelle et al. (2020) does not change the flowing regime of the power during the collision.

3. Results and discussion

3.1 Dynamic ball indentation results

The data of the dynamic ball indentation is reported in Figure 2 for the indenters with two different diameters. In x-axis, the dimensionless shear rate is reported and it was calculated as follows:

$$\dot{\gamma}^* = \dot{\gamma}\sqrt{\frac{d_p}{g}} \quad (8)$$

The dynamic hardness instead is reported in the y-axis and it was calculated using Eq(6). The magnitude of the dimensionless shear rate gives information about the flowing condition of powders: when $\dot{\gamma}^*$ is between 0.15 and 0.20 the material is considered to be in the *quasi-static frictional regime* of flow; when it is between 0.25 and 3 the powder is in the *intermediate regime* where friction but also collisions between particles must be considered, with the combination from collisions increasing with shear rate.

Finally, for dimensionless shear rates beyond 3, the powder is in the *dynamic regime* of flow. Here, rapid and short-duration collisions are predominant, individual powder particles are sufficiently energized and the powder behaves like a freely flowing fluid (Tardos et al., 2003). In this classification, the boundaries between regimes are still uncertain and not clearly defined (Tardos et al, 2003). The experimental data in Figure 2 shows that the powder always flows in the intermediate regime, where friction and collisions can occur. It appears that the dynamic hardness increases when the dimensional shear rate increases. In a previous work (Tirapelle et al., 2020), the authors observed the dynamic hardness remained constant with the shear rate, when the powder was in *quasi-static* regime. Both the observations are in agreement with what was observed by Tardos (2003), who observed that a power law fitted their data (shear stress and normal stress vs dimensionless shear rate).
The power law that best fits the curve has an exponent equal to *n*=1.98, according to the fit found by Tardos et al. (2003) in the *intermediate regime.*

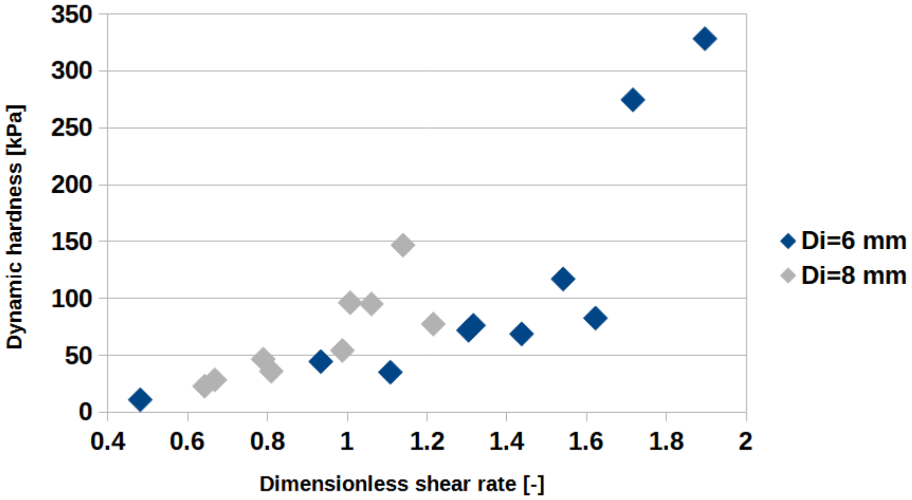

Figure 2: Dynamic hardness plotted versus the dimensionless shear rate at different indenters.

3.2 Determination of the operating conditions

Tirapelle et al. (2020) found a dimensionless correlation that fitted all the indenter data. In their study, four different powders, at different consolidation states and different types of indenters were used.
They defined four dimensionless groups that control the dynamic indentation: (1) the ratio between the bulk density and the intrinsic density of the indenter; (2) the ratio between the crater radius and the diameter of the powder; (3) the ratio between the penetration depth and the indenter radius and (4) the ratio between the inertial and the hydrostatic stresses which are representative of the stress state in the powder during and before indentation respectively.
It was found that the product of the four groups elevated to an appropriate exponent as follows:

$$b = \left(\frac{\rho_b}{\rho_i}\right)^{0.5} \left(\frac{R_c}{d_p}\right) \left(\frac{h}{R_i}\right)^{1.5} \left(\frac{\rho_b \dot{\gamma}^2 d_p^2}{\rho_b g h}\right) \quad (9)$$

makes all the data collapse on a master curve if plotted against the dimensionless shear rate as shown in Figure 3.
Manipulation of the four groups using their fitted exponents leads to further simplifications of the geometrical and dynamic groups, resulting in the following simple expression:

$$b = \left(\frac{\rho_b}{\rho_i}\right)^{0.5} h^*\left(2 - h^*\right)^{0.5} \gamma^{*2} \quad (10)$$

where h^* is the dimensionless penetration depth calculated as the ratio between h and R_i.
The dimensionless expression for b works well also using the shear rate as defined in Eq(7). This line has a positive slope, therefore achieving larger values of dimensionless shear rate, requires a more consolidate powder, larger particles dimensions or larger indenter impact speed.

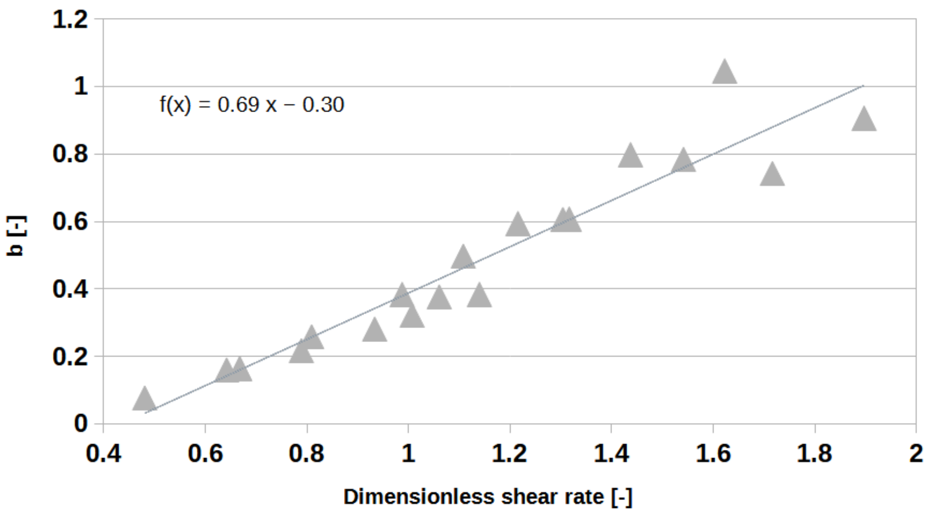

Figure 3: The dimensionless number in Eq(10) calculated for all the dynamic hardness measurements, done f or this work, is represented as a function of the dimensionless shear rate. All the observations are fitted by linear regression.

The proposed relationship is useful for predicting the best applicable operative conditions for dynamic indentation tests. For instance, because usually the indenter, the powder properties, and the desired dimensionless shear rate are known, one could find the dimensionless penetration depth, h^*, with the help of Figure 3. Currently one can calculate the penetration depth, the impact velocity and hence the required drop height (Tirapelle et al, 2020).

3.3 Dynamic hardness and packing fractions

As last analysis, we tried to link the dynamic hardness of the powder with the initial consolidation of the powder. Hence, the packing fraction was calculated as follows:

$$\nu = \frac{\rho_b}{\rho_g} \quad (11)$$

where ρ_g is the intrinsic density of sodium bicarbonate.

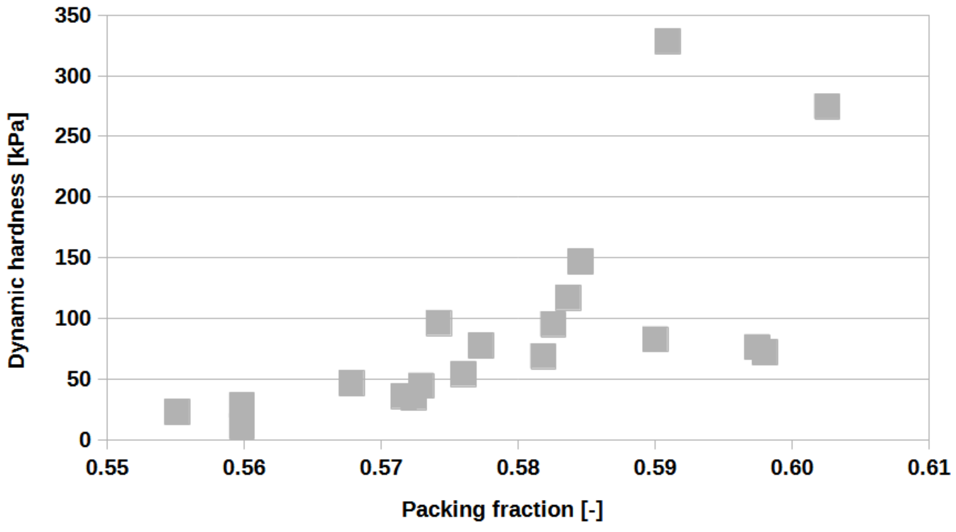

Figure 4: Variation of the dynamic hardness with packing fraction of the bed.

Figure 4 shows how the packing fraction of the bed influences the resistance to the plastic deformation of the powder by the action of the indenter. Packing fraction indeed directly affects the ability of the individual particles to move and reorganize their position in the bed in response to the impact. For packing fractions lower than 0.59 the data follows a unique trend. For packing fractions greater than 0.59, instead, the dynamic hardness shows two different regimes; for the same packing density, in fact, two different hardness values are calculated. The points at larger hardness (ranging between 250 and 350 kPa) also presented the greatest value of granular velocity, greater than 3 m/s. The lower points that present a hardness value about 50 kPa are obtained with granular velocity less than 1 m/s.

4. Conclusions

This experimental work proposes an alternative experimental method to determine the flowability of the powder. The method, called *Dynamic Ball Indentation* method, consists of dropping a ball of known density and diameter onto a bed of powder in a known state of consolidation. The resistance of the powder to the impact is calculated through the hardness calculated based on the impact velocity of the indenter. In this work we proposed an alternative expression for dynamic hardness based on the powder velocity. Furthermore, also the shear rate was calculated using the powder velocity. We also shown that a dimensionless equation useful for determining the operating condition of the indentation was still valid when inserted the new equation for the shear rate proposed. Ultimately, we had shown a relation between the dynamic hardness and the packing fraction of the powder. The packing fraction, in fact, results one of the properties that strongly affects the hardness variation.

Nomenclature

A – penetration area, m^2
b – ,dimensional number
d_p – particle diameter, m
D_i – indenter diameter, m
F_{max} – maximum loading force, N
g – gravity acceleration, m/s
h – penetration depth, m
h_d – drop height, m
H_d – dynamic hardness, kPa
H_s – quasi-static hardness, kPa
m_i– indenter mass, kg
R_c – crater radius, m
U – crater volume, m^3
v_i – impact velocity, m/s
v_g – granular velocity, m/s
$\dot{\gamma}$ – shear rate,1/s
$\dot{\gamma}^*$ – dimensionless shear rate
ρ_b – powder bulk density , kg/m^3
ρ_g - intrinsic powder density,.kg/m^3
ρ_i - indenter density, kg/m^3
ν - packing density

References

Hassanpour A., Ghadiri M., 2007, Characterisation of flowability of loosely compacted cohesive powders by indentation, Particle & Particle Systems Characterization, 24(2), 117-123
Pasha M., Hare C., Hassanpour A., Ghadiri, M, 2015, Numerical analysis of strain rate sensitivity in ball indentation on cohesive powder Beds, Chemical Engineering Science, 123, 92-98
Tardos G. I., McNamara S., Talu I., 2003, Slow and intermediate flow of a frictional bulk powder in the Couette geometry, Powder Technology, 131(1), 23-39.
Tirapelle M., Santomaso A. C., Hare C, 2020, Dynamic ball indentation for powder flow characterization, Powder Technology, 360, 1047-1054
Tirupataiah Y., Sundararajan G., 1991, A dynamic indentation technique for the characterization of the high strain rate plastic flow behaviour of ductile metals and alloys, Journal of the Mechanics and Physics of Solids, 39(2), 243-271
Zafar U., Hare C., Calvert G., Ghadiri M., Girimonte R., Formisani B., Valverde J. M., 2015, Comparison of cohesive powder flowability measured by Schulze shear cell, raining bed method, Sevilla powder tester and new ball indentation method, Powder Technology, 286, 807-816